Tetracoordinated Planar Carbon in the Al_4C^- Anion. A Combined Photoelectron Spectroscopy and ab Initio Study

Xi Li,[†] Lai-Sheng Wang,*[,†] Alexander I. Boldyrev,*[,‡,§] and Jack Simons*[,‡]

Contribution from the Department of Physics, Washington State University, Richland, Washington 99352, the Environmental Molecular Sciences Laboratory, Pacific Northwest National Laboratory, MS K8-88, P.O. Box 999, Richland, Washington 99352, and the Department of Chemistry, The University of Utah, Salt Lake City, Utah 84112

Received February 26, 1999

Abstract: The chemical structure and bonding of Al_4C and Al_4C^- have been studied by photoelectron spectroscopy and ab initio calculations. While Al_4C is known to be a tetrahedral molecule, the data reported here suggest that Al_4C^- has D_{4h} symmetry (when averaged over zero-point vibrational motions) and thus is the smallest species identified to date that contains a tetracoordinated planar carbon atom. The experimental vertical electron detachment energy of Al_4C^- (2.65 ± 0.06 eV) compares well to 2.71 eV calculated at the CCSD(T)/6-311+G(2df) level of theory. The excellent agreement between the calculated and experimental electron detachment energies, excitation energies, and other spectral features allows us to elucidate the structure of the tetracoordinated planar-carbon-containing Al_4C^- anion.

Introduction

The basis of the most successful stereochemical concept in organic chemistry, that of the tetravalent tetrahedral carbon atom, was published in 1874 independently by van't Hoff[1] and LeBel.[2] The possibility of designing molecules containing a planar tetracoodinated carbon atom, a task that requires overcoming the inherent preference for tetrahedral bonding, has been pursued for some considerable time.[3−15] Two approaches to achieving this goal have been employed. The electronic approach involves selecting substituents that will preferentially stabilize a planar disposition of the carbon bonds over the normal tetrahedral arrangement.[4−10] The alternative approach is based on using mechanical forces exerted by the surrounding ligands bound to the carbon atom.[11−15] In the present efforts we consider a species for which the electronic effects are most important.

Recently, a set of pentaatomic molecules, *cis*-CSi_2Al_2, *trans*-CSi_2Al_2, *cis*-CSi_2Ga_2, *trans*-CSi_2Ga_2, *cis*-CGe_2Al_2, and *trans*-

[†] Washington State University and Pacific Northwest National Laboratory.

[‡] The University of Utah.

[§] Present adress: Department of Chemistry and Biochemistry, Utah State University, Logan, UT 84322-0300.

(1) van't Hoff, J. H. *Arch. Neerl. Sci. Exactes Nat*. **1874**, 445.

(2) LeBel, J. A. *Bull. Soc. Chim. Fr*. **1874**, *22*, 337.

(3) For reviews on this topic see: (a) Liebman, J. F.; Greenberg, A. *Chem. Rev*. **1976**, *76*, 311. (b) Greenberg, A.; Liebman, J. F. *Strain Organic Molecules*; Academic Press: New York, 1978. (c) Keese, R. *Nachr. Chem. Technol. Lab*. **1982**, *30*, 844. (d) Veneoalli, B. R.; Agosta, W. C. *Chem. Rev*. **1987**, *87*, 399. (e) Erker, G. *Comments Inorg. Chem*. **1992**, *13*, 111. (f) Agosta, W. C. In *The Chemistry of Alkanes*; J. Wiley: New York, 1992; Chapter 20. (g) Erker, G. *Nachr. Chem. Technol. Lab*. **1992**, *40*, 1099. (h) Luef, W.; Keese, R. *Adv. Strain Org. Chem*. **1993**, *3*, 229. (i) Luef, W.; Keese, R. *Adv. Strain. Chem*. **1993**, *3*, 329. (j) Sorger, K.; Schleyer, P. v. R. *J. Mol. Struct*. **1995**, *338*, 317. (k) Rottger, D.; Erker, G. *Angew. Chem., Int. Ed. Engl*. **1997**, *36*, 812.

(4) (a) Hoffmann, R.; Alder, R. W.; Wilcox, C. F., Jr. *J. Am. Chem. Soc*. **1970**, *92*, 4992. (b) Hoffmann, R. *Pure Appl. Chem*. **1971**, *28*, 181.

(5) (a) Collins, J. B.; Dill, J. D.; Jemmis, E. D.; Apeloig, Y.; Schleyer, P. v. R.; Seeger, R.; Pople, J. A. *J. Am. Chem. Soc*. **1976**, *98*, 5419. (b) Krogh-Jesperson, M. B.; Cremer, D.; Poppinger, D.; Pople, J. A.; Schleyer, P. v. R.; Chandrasekhar, J. *J. Am. Chem. Soc*. **1979**, *101*, 4843. (c) Chadrasekhar, J.; Wurthwein, E. U.; Schleyer, P. v. R. *Tetrahedron* **1981**, *37*, 921.

(6) (a) Schleyer, P. v. R.; Boldyrev, A. I. *J. Chem. Soc., Chem. Commun*. **1991**, 1536. (b) Boldyrev, A. I.; Simons, J. *J. Am. Chem. Soc*. **1998**, *120*, 7967.

(7) (a) Laidig, W. D.; Schaefer, H. F., III *J. Am. Chem. Soc*. **1978**, *100*, 5972. (b) Bohm, M. C.; Gleiter, R.; Schlang, P. *Tetrahedron Lett*. **1979**, 2675.

(8) (a) Cotton, F. A.; Millar, M. *J. Am. Chem. Soc*. **1977**, *99*, 7886. (b) Cotton, F. A.; Lewis, G. F.; Mott, G. N. *Inorg. Chem*. **1983**, *22*, 560.

(9) (a) Erker, G.; Albrecht, M.; Kruger, C.; Wener, S. *Organometallics* **1991**, *10*, 3791. (b) Albrecht, M.; Erker, G.; Notle, M.; Kruger, C. *J. Organomet. Chem*. **1992**, *427*, C21. (c) Erker, G.; Albrecht, M.; Wener, S.; Notle, M.; Wener, S.; Binger, P.; Langhauser, F. *Organometallics* **1992**, *11*, 3517. (d) Erker, G.; Albrecht, M.; Kruger, C.; Wener, S. *J. Am. Chem. Soc*. **1992**, *114*, 8531. (e) Gleiter, R.; Hyla-Kryspin, I.; Niu, S.; Erker, G. *Angew. Chem., Int. Ed. Engl*. **1993**, *32*, 754. (f) Poumbga, C. N.; Bernar, M.; Hyla-Kryspin, I. *J. Am. Chem. Soc*. **1994**, *116*, 8259. (g) Rottger, D.; Erker, G.; Frohlich, R.; Grehl, M.; Silverio, S. J.; Hyla-Kryspin, I.; Gleiter, R. *J. Am. Chem. Soc*. **1995**, *117*, 10503. (h) Hyla-Kryspin, I.; Gleiter, R.; Romer, M.-M.; Deveny, J.; Gunale, A.; Pritzkow, H.; Siebert, W. *Chemistry* **1997**, *2*, 294.

(10) (a) Bachrach, S. M.; Streitweiser, A., Jr. *J. Am. Chem. Soc*. **1984**, *106*, 5818. (b) Frenking, G. *Chem. Phys. Lett*. **1984**, *111*, 529. (c) Glukhovtsev, M. N.; Simkin, B. Ya.; Minkin, V. I. *J. Org. Chem. USSR* **1990**, *26*, 1933. (d) Glukhovtsev, M. N.; Simkin, B. Ya.; Minkin, V. I. *J. Org. Chem. USSR* **1991**, *27*, 1. Glukhovtsev, M. N.; Pross. A.; Radom, L. *J. Am. Chem. Soc*. **1994**, *116*, 5961.

(11) (a) Wiberg, K.; Hiatt, J. E.; Burgmaier, G. *Tetrahedron Lett*. **1968**, 5855. (b) Wiberg, K. B.; Elison, G. B.; Wendolski, J. J. *J. Am. Chem. Soc*. **1976**, *98*, 1212. (c) Wiberg, K. B.; Odonnell, *J. Am. Chem. Soc*. **1979**, *101*, 6660. (d) Wiberg, K. B.; Olli, L. K.; Golembeski, N.; Adams, R. D. *J. Am. Chem. Soc*. **1980**, *102*, 7467. (e) Wiberg, K. B.; Wendoloski, J. J. *J. Am. Chem. Soc*. **1982**, *104*, 5679. (f) Wiberg, K. B. *Tetrahedron Lett*. **1985**, *26*, 5967.

(12) (a) Krogh-Jesperson, M. B.; Chandrasekhar, J.; Wurthwein, E. U.; Collins, J. B.; Schleyer, P. v. R. *J. Am. Chem. Soc*. **1980**, *102*, 2263. (b) Wurthwein, E. U.; Chadrasekhar, J.; Jemmis, E. D.; Schleyer, P. v. R. *Tetrahedron Lett*. **1981**, *22*, 843.

(13) (a) Keese, R.; Pfenninger, A.; Roesle, A. *Helv. Chim. Acta* **1979**, *62*, 326. (b) Schori, H.; Patil, B. B.; Keese, R. *Tetrahedron* **1981**, *37*, 4457. (c) Thommen, M.; Gerber, P.; Keese, R. *Chimia* **1991**, *45*, 21. (d) Luef, W.; Keese, R. *J. Mol. Struct. (THEOCHEM)* **1992**, *257*, 353.

(14) (a) Dodziuk, H. *Bull. Chem. Soc. Jpn*. **1987**, *60*, 3775. (b) Dodziuk, H. *J. Mol. Struct*. **1990**, *239*, 167.

(15) (a) McGrath, M. P.; Schaefer, H. F., III; Radom, L. *J. Org. Chem*. **1992**, *57*, 4847. (b) McGrath, M. P.; Radom, L. *J. Am. Chem. Soc*. **1993**, *115*, 3320.

10.1021/ja9906204 CCC: $18.00
Published on Web 00/00/0000 PAGE EST: 5.5

CGe_2Al_2, with tetracoordinated planar carbon have been predicted computationally.[6] In such species, bonding interactions between the central carbon and the ligands and among the ligands are *both* important in favoring the planar arrangement. We believe that understanding the bonding in such molecules is crucial to future progress in designing novel molecules and compounds with tetracoordinated planar carbon.

It is shown in ref 6 that the stability of the predicted planar tetracoordinated carbon species is related to the occurrence of 18 valence electrons, which produce three σ and one π bonds to the central carbon atom plus one four-center ligand−ligand bond, and four ligand-centered lone pairs.[6b] According to the model of ref 6, 16-valence-electron species such as Al_4C will not be stable at D_{4h} symmetry because they lack the ligand−ligand bond. Indeed for such species, the planar structure has been found to be less stable then the tetrahedral.[6a] Although the situations for 18 and 16 electrons have been resolved, the 17-electron case remains to be addressed.

In the current work, we present a combined experimental and theoretical study on a 17-valence-electron pentaatomic species, Al_4C^-. We demonstrate that the combination of anion photoelectron spectroscopy (PES) and high-level ab initio calculations can completely elucidate the structures of both Al_4C^- and the neutral Al_4C. Our findings confirm that the 16-electron Al_4C is indeed tetrahedral, and show that the 17-electron Al_4C^- is actually planar. To the best of our knowledge, there are no other experimental data available on Al_4C^- and Al_4C, although a number of other hyperaluminum molecules, Al_3O,[16−20] Al_4O,[17,21] Al_nN ($n = 3, 4$),[21,22] and Al_nS ($n = 3-9$),[23] have been studied in the literature. The substantial stability of the later molecules is due to the high degree of ionic character in the bonding between the central atom and its ligands, as well as the bonding interactions among the ligand aluminum atoms.[17]

Experimental Methods

The experiments were performed with a magnetic-bottle time-of-flight PES apparatus. Details of the experiment have been described previously.[24,25] Briefly, Al_4C^- was produced by a laser vaporization cluster source. An intense laser pulse (532 nm) from a Q-switched Nd:YAG laser was focused onto a pure Al target. Sufficient Al_4C^- mass signals were produced due to carbon impurity in the Al target. A mixed Al/C target was also used, but it favored clusters with high C content ($Al_4C_x^-$, $x > 1$) and Al_4C^- was not produced more abundantly. The clusters formed from the laser vaporization source were entrained in a He carrier gas and underwent a supersonic expansion. The anion species in the beam were extracted perpendicularly into a time-of-flight mass spectrometer. The Al_4C^- anions were selected and decelerated before photodetachment by a laser beam. For the current experiment, three detachment photon energies were used, 355 (3.496 eV), 266 (4.661 eV), and 193 nm (6.424 eV). The electron kinetic energy resolution of the apparatus was better than 30 meV for 1 eV electrons at 355 and 266 nm and it deteriorated at 193 nm.

Computational Methods

We initially optimized the geometries of Al_4C and Al_4C^- employing analytical gradients with polarized split-valence basis sets (6-311+G*)[26−28] using the hybrid method, which includes a mixture of Hartree−Fock exchange with density functional exchange correlation (B3LYP).[29−31] Then, the geometries were refined at the MP2 level of theory[32] with the 6-311+G* basis sets. For the most stable structures resulting from those initial considerations, we also employed the CCSD(T) method[33−35] and the same basis sets to even better determine the geometries. Finally, the energies of the lowest energy structures were refined by using the CCSD(T) level of theory and the more extended 6-311+G(2df) basis sets. All core electrons were kept frozen in treating the electron correlation at the MP2 and the CCSD(T) levels of theory, and all calculations were performed with the Gaussian-94 program.[36]

Experimental Results

The PES spectra of Al_4C^- are shown in Figure 1 at three photon energies. The 355-nm spectrum (Figure 1a) shows a broad low-energy tail (X) and two intense and sharp features with 2.86 (A) and 3.00 eV (B) vertical (inferred from peak energies) binding energies (VDEs), respectively. A weak feature (C) at 3.3 eV VDE is also discernible. At 266 nm (Figure 1b), the broad low-energy tail (X) was enhanced and became a well-defined feature with a VDE at 2.65 eV. The C feature was also observed more clearly in the 266-nm spectrum. Additional higher energy broad features were observed at 266 nm. Two features (D and E) could be roughly identified at ~3.7 and 4.2 eV VDEs. The 193-nm spectrum (Figure 1c) seems to reveal more transitions at high binding energies beyond 4.4 eV, but they are broad and congested.

The PES spectra of Al_4C^- are rather complicated. The broad low-energy feature (X) was unusual and could be due to several sources. It could be due to hot band transitions, excited states of anions, or minor isomers, all of which should depend on the cluster source conditions to some degree. However, this broad tail always existed even when source conditions were changed slightly to produce colder clusters. Therefore, we concluded that, even though there could be contributions due to hot bands to the broad feature (X), the main intensity of this feature was due to the transition from the ground state of the anion to that of the neutral ground state. This suggests a large geometry

(16) Cox, D. M.; Trevor, D. J.; Whitten, R. L.; Rohlfing, E. A.; Kaldor, A. *J. Chem. Phys.* **1986**, *84*, 4651.
(17) Boldyrev, A. I.; Schleyer, P. v. R. *J. Am. Chem. Soc*. **1991**, *113*, 9045.
(18) Zakrzewski, V. G.; Niessen, W. von; Boldyrev, A. I.; Schleyer, P. v. R. *Chem. Phys. Lett*. **1992**, *197*, 195.
(19) Wu, H.; Li, X.; Wang, X. B.; Ding, C. F.; Wang, L. S. *J. Chem. Phys*. **1998**, *109*, 449.
(20) Jarrold, M. F.; Bower, J. E. *J. Chem. Phys*. **1987**, *87*, 1610.
(21) Zakrzewski, V. G.; Niessen, von W.; Boldyrev, A. I.; Schleyer, P. v. R. *Chem. Phys. Lett*. **1993**, *174*, 167.
(22) Nayak, S. K.; Rao, B. K.; Jena, P.; Li, X.; Wang, L. S. *Chem. Phys. Lett*. **1999**, *197*, 195.
(23) Nakajima, A.; Taguwa, T.; Nakao, K.; Hoshino, K.; Iwata, S.; Kaya, K. *J. Chem. Phys*. **1995**, *102*, 660.
(24) Wang, L. S.; Cheng, H. S.; Fan, J. *J. Chem. Phys*. **1998**, *102*, 9480.
(25) Wang, L. S.; Wu, H. In *Advances in Metal and Semiconductor Clusters. IV. Cluster Materials*; Duncan, M. A., Ed.; JAI Press: Greenwich, 1998; pp 299−343.
(26) McLean, A. D.; Chandler, G. S. *J. Chem. Phys*. **1980**, *72*, 5639.
(27) Clark, T.; Chandrasekhar, J.; Spitznagel, G. W.; Schleyer, P. v. R. *J. Comput. Chem*. **1983**, *4*, 294.
(28) Frisch, M. J.; Pople, J. A.; Binkley, J. S. *J. Chem. Phys*. **1984**, *80*, 3265 1984.
(29) Parr, R. G.; Yang, W. *Density-functional theory of atoms and molecules*; Oxford University Press: Oxford, 1989.
(30) Becke, A. D. *J. Chem. Phys*. **1992**, *96*, 2155.
(31) Perdew, J. P.; Chevary, J. A.; Vosko, S. H.; Jackson, K. A.; Pederson, M. R.; Singh, D. J.; Fiolhais, C. *Phys. Rev. B* **1992**, *46*, 6671.
(32) Krishnan, R.; Binkley, J. S.; Seeger, R.; Pople, J. A. *J. Chem. Phys*. **1980**, *72*, 650.
(33) Cizek, J. *Adv. Chem. Phys*. **1969**, *14*, 35.
(34) Purvis, G. D., III; Bartlett, R. J. *J. Chem. Phys*. **1982**, *76*, 1910.
(35) Scuseria, G. E.; Janssen, C. L.; Schaefer, H. F., III *J. Chem. Phys*. **1988**, *89*, 7282.
(36) *GAUSSIAN 94*, Revision A.1; Frisch, M. J.; Trucks, G. W.; Schlegel, H. B.; Gill, P. M. W.; Johnson, B. G.; Robb, M. A.; Cheeseman, J. R.; Keith, T. A.; Peterson, G. A.; Montgomery, J. A.; Raghavachari, K.; Al-Laham, M. A.; Zakrzewski, V. G.; Ortiz, J. V.; Foresman, J. B.; Cioslowski, J.; Stefanov, B. B.; Nanayakkara, A.; Challacombe, M.; Peng, C. Y.; Ayala, P. Y.; Chen, W.; Wong, M. W.; Anders, J. L.; Replogle, E. S.; Gomperts, R.; Martin, R. L.; Fox, D. J.; Binkley, J. S.; DeFrees, D. J.; Baker, J.; Stewart, J. J. P.; Head-Gordon, M.; Gonzalez, C.; Pople J. A.; Gaussian Inc.: Pittsburgh, PA, 1995.

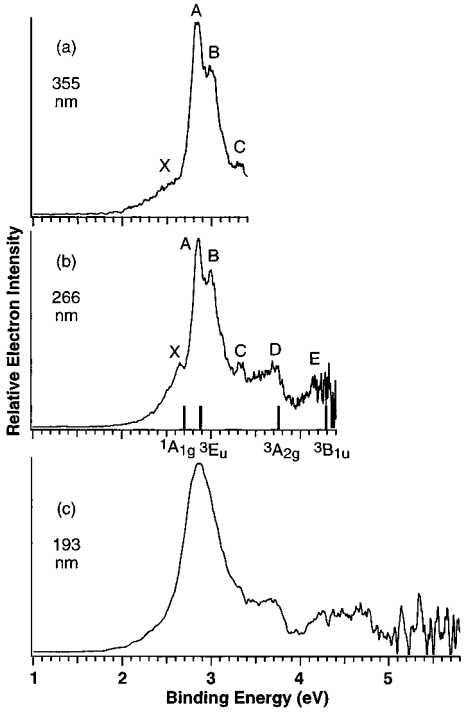

Figure 1. Photoelectron spectra of Al_4C^- at (a) 355 (3.496 eV), (b) 266 (4.661 eV), and (c) 193 nm (6.424 eV). The observed detachment channels are labeled X, A, B, C, D, and E. The vertical lines in part b represent the calculated vertical electron binding energies of the four major detachment channels (see Table 4).

Table 1. Calculated Molecular Properties of the Tetrahedral Al_4C Molecule

property	B3LYP/ 6-311+G*	MP2/ 6-311+G*	CCSD(T)/ 6-311+G*
$R(C-Al_{2,3,4,5})$, Å	2.010	2.002	1.999
$R(Al_2-Al_3)$, Å	3.282	3.270	3.265
E_{tot}, au	−1007.868295	−1005.848076	−1005.914193
$\nu_1(a_1)$, cm^{-1}	350	359	363
$\nu_2(e)$, cm^{-1}	97	96	95
$\nu_3(t_2)$, cm^{-1}	610	637	640
$\nu_4(t_2)$, cm^{-1}	170	175	175

change between the anion and the neutral ground state. There are additional factors causing the complicated PES spectra of Al_4C^-, which possesses an odd number of valence electrons and can lead to states with more complicated spin multiplicities as discussed below.

Theoretical Results

Al_4C. At all three levels of theory, B3LYP/6-311+G*, MP2/6-311+G*, and CCSD(T)/6-311+G*, the global minimum of Al_4C was found to have a singlet T_d ($^1A_1$) structure (characterized in Table 1 and shown in Figure 2) in agreement with the previous MP2(full)/6-31G* calculations.[6a] The optimal geometries and harmonic frequencies are consistent at all levels of theory. The tetrahedral structure of Al_4C is to be expected[6] based on the occupations of the valence MOs in the 32-valence-electron *tetrahedral* CF_4 molecule, $1a_1^2 1t_2^6 2a_1^2 2t_2^6 1e^4 3t_2^6 1t_1^6$. The first four ($1a_1^2$ and $1t_2^6$) orbitals are the C−F σ bonds and the remaining 12 orbitals are lone-pair orbitals localized on F atoms, lying perpendicular and parallel to the C−F bond axes. The above orbital occupancy clearly describes a situation with four σ bonds and no net bonding or antibonding interactions among the ligands. If we assume that this order of MOs remains

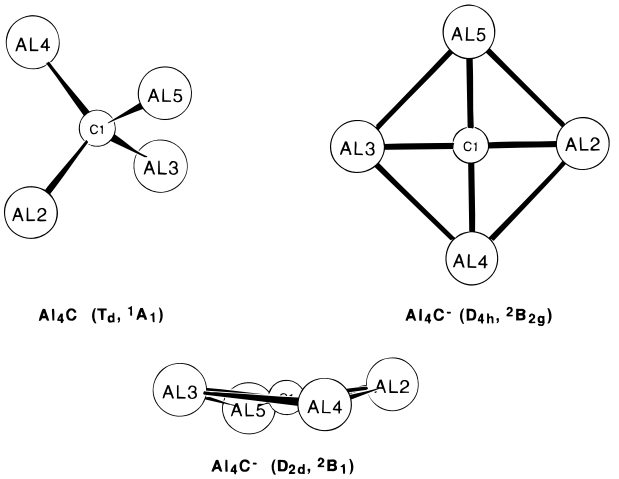

Figure 2. Optimized Al_4C and Al_4C^- structures. See Tables 1−3 for structural parameters.

Table 2. Calculated Molecular Properties of the D_{4h} ($^2B_{2g}$) Structure of Al_4C^-

property	B3LYP/ 6-311+G*	MP2/ 6-311+G*	CCSD(T)/ 6-311+G*
$R(C-Al_{2,3,4,5})$, Å	1.993	1.993	1.992
$R(Al_2-Al_4)$, Å	2.819	2.819	2.817
E_{tot}, au	−1007.936385	−1005.912335	−1005.971282
$\nu_1(a_{1g})$, cm^{-1}	374	383	384
$\nu_2(a_{2u})$, cm^{-1}	210	29	59*i*
$\nu_3(b_{1g})$, cm^{-1}	287	307	305
$\nu_4(b_{2g})$, cm^{-1}	207	230	227
$\nu_5(b_{2u})$, cm^{-1}	53	26	47*i*
$\nu_6(e_u)$, cm^{-1}	602	791	660
$\nu_7(e_u)$, cm^{-1}	42	247	142

valid for other tetrahedral molecules, for example, for a species with 16 valence electrons such as Al_4C, the tetrahedral structure should have a $1a_1^2 1t_2^6 2a_1^2 2t_2^6 1e^0$ electronic configuration, which describes four σ bonds ($1a_1$ and $1t_2$) and four lone-pair bonds ($2a_1$ and $2t_2$).[6b] This result suggests that each Al in Al_4C can be viewed as monovalent with a 3s lone pair.

Al_4C^-. Addition of an electron to the 1e LUMO of T_d Al_4C, which consists of Al 3p orbitals lying perpendicular to the Al−C bond axes, leads to a $1a_1^2 1t_2^6 2a_1^2 2t_2^6 1e^1$ electronic configuration with a ^2E state for Al_4C^-, which is expected to undergo Jahn−Teller distortion toward a D_{4h} ($^2B_{2g}$) geometry (Figure 2). We optimized the D_{4h} structure ($^2B_{2g}$, $1a_{1g}^2 1e_u^4 2a_{1g}^2 1a_{2u}^2 1b_{1g}^2 2e_u^4 1b_{2g}^1 1e_g^0$) at the above three levels of theory (see Table 2 for final geometry parameters) and found the D_{4h} ($^2B_{2g}$) state to be a minimum at the B3LYP/6-311+G* and MP2/6-311+G* levels of theory, but a second-order saddle point at the CCSD(T)/6-311+G* level of theory. Distortion along the a_{2u} mode of imaginary frequency leads to a C_{4v} ($^2B_1$) pyramidal (but almost planar) structure with the carbon atom lying just 0.0056 Å above the Al_4 plane and with an inversion barrier of only 0.002 kcal/mol. Distortion along the b_{2u} mode of imaginary frequency leads to a butterfly type D_{2d} ($^2B_1$) structure (Figure 2 and Table 3), which turns out to be the global minimum at the CCSD(T)/6-311+G* level of theory. However, the deviation from planarity in the butterfly structure is also rather small with the energy difference between D_{2d} ($^2B_1$) and D_{4h} ($^2B_{2g}$) being 0.14 kcal/mol. Therefore, when zero-point vibrational motion is considered, *the vibrationally averaged structure is actually planar*.

The propensity of 17- and 18-valence-electron pentaatomic systems to achieve planarity can be understood by considering of the $1b_{2g}$ HOMO (Figure 3), which is clearly bonding with

Table 3. Calculated Molecular Properties of the C_{4v} ($^2B_1$) Saddle Point and the D_{2d} ($^2B_1$) Global Minimum of the Al_4C^- Anion

	CCSD(T)/6-311+G*	
property	D_{2d}	C_{4v}
R(C−$Al_{2,3,4,5}$), Å	1.990	1.992
R(Al_2−Al_4), Å	2.827	2.816
∠Al_2CAl_3, deg	169.2	176.2
E_{tot}, au	−1005.971512	−1005.671286

respect to ligand−ligand interactions and plays a key role in maintaining planarity. Why the Al_4C^- anion is not exactly planar most likely has to do with the size of the "cavity" in the planar Al_4 cluster; a similar observation was made in the CSi_2Al_2 case.[6b] To achieve perfect planarity one could use isoelectronic but larger ligands such as Ga or In in place of Al. Thus, we expect that planar (or quasiplanar) structures will also occur in $CAl_2Ga_2^-$, CGa_4^-, and neutral 17-valence-electron species such as CAl_3Si, CAl_2GaSi, $CAlGa_2Si$, CGa_3Si, CAl_3Ge, etc.

Alternative Structures. For both the neutral Al_4C and Al_4C^- we also considered other structures with different spin multiplicities and geometries.

For the triplet state of Al_4C, we do not expect a tetrahedral structure because the $1a_1^2 1t_2^6 2a_1^2 2t_2^5 1e^1$ electronic configuration is not stable toward Jahn−Teller distortion. We performed geometry optimization for this triplet state of Al_4C without any symmetry restriction which generated a local minimum planar structure C_{2v}, $^3B_2$ ($1a_1^2 2a_1^2 1b_2^2 3a_1^2 1b_1^2 4a_1^2 2b_2^2 5a_1^1 3b_2^1$) 1.01 eV (MP2/6-311+G*) higher in energy than the singlet tetrahedral structure.

Next, we considered structures with one Al atom coordinated outside a CAl_3 cluster. Geometry optimization of the $AlCAl_2$-Al (C_{2v}, $^1A_1$) structure within C_{2v} symmetry converged to a D_{4h}, $^1A_{1g}$ structure which is a saddle point 0.85 eV (MP2/6-311+G*) higher in energy than the singlet tetrahedral structure. Geometry optimization of the CAl_3Al (C_{3v}, $^1A_1$) structure with the carbon atom coordinated to a face of a tetrahedral Al_4 cluster within C_{3v} symmetry converged to the T_d, $^1A_1$ structure. Therefore, all alternative structures were found to be higher in energy than the T_d, $^1A_1$ structure from which we conclude that the T_d, $^1A_1$ structure detailed in Table 1 and Figure 2 is the global minimum for the Al_4C molecule.

For the quartet state of Al_4C^- we do not expect a D_{4h} structure because the $1a_{1g}^2 1e_u^4 2a_{1g}^2 1a_{2u}^2 1b_{1g}^2 2e_u^3 1b_{2g}^1 1e_g^1$ electronic configuration is not stable toward Jahn−Teller distortion. We performed geometry optimization for this quartet state of Al_4C^- without any symmetry restriction which converged to a C_{3v}, $^4A_1$ ($1a_1^2 2a_1^2 1e^4 3a_1^2 2e^4 4a_1^1 3e^2$) local minimum structure, which is 1.72 eV (MP2/6-311+G*) higher in energy than the doublet D_{4h} ($^2B_{2g}$) structure.

Next, we considered anion structures with one Al atom coordinated outside the CAl_3 cluster. Geometry optimization of the $AlCAl_2Al^-$ (C_{2v}, $^2B_1$) structure within C_{2v} symmetry converged to the D_{4h}, $^2B_{2g}$ structure. Geometry optimization of a $AlCAl_2Al^-$ (C_{2v}, $^4B_1$) structure within C_{2v} symmetry converged to a structure, which is a second-order saddle point, 2.05 eV higher in energy than the D_{2h} ($^2B_{2g}$) structure. Therefore, all alternative structures were found to be higher in energy than the D_{2h} ($^2B_{2g}$) structure, and we conclude that the D_{2d} ($^2B_1$) structure detailed in Table 3 and Figure 2 is the global minimum for the Al_4C^- anion.

Both the D_{2d} Al_4C^- anion and the T_d Al_4C neutral molecule are very stable toward dissociation. Representative dissociation energies were calculated to be as follows: $\Delta E = 2.41$ eV for Al_4C^- (D_{2d}, $^2B_1$) → Al_3C^- (C_{3v}, $^1A_1$) + Al (^2P) and $\Delta E = 3.05$ eV for Al_4C (T_d, $^1A_1$) → Al_3C (C_{2v}, $^2B_2$) + Al (^2P) (all at the CCSD(T)/6-311+G(2df) level of theory).

Interpretation of the Experimental Spectra

The deviation from planarity in Al_4C^- is below the ZPE corrections and therefore we consider that electron detachment occurs from the D_{4h} ($^2B_{2g}$) planar structure in our interpretation of the experimental photoelectron spectra. In Table 4 we present the results of our calculations of the four major low-lying vertical one-electron detachment processes from the D_{4h} ($^2B_{2g}$) state of Al_4C^-. The four calculated detachment channels are also shown in Figure 1b as vertical bars.

Feature X. The lowest vertical electron detachment should occur by electron removal from the $1b_{2g}$-HOMO. The broad feature X (Figure 1) peaking at 2.65 ± 0.06 eV agrees well with the calculated VDE of 2.71 eV [CCSD(T)/6-311+G(2df)] from the $1b_{2g}$-HOMO. The $1b_{2g}$-orbital (Figure 3) is a ligand−ligand bonding MO composed primarily of 3s and 3p atomic orbitals (AOs) of the aluminum atoms. Therefore, we assign feature X to the (X, Al_4C^-) → (X, Al_4C) transition. The broad nature of this transition is consistent with the fact that neutral Al_4C is tetrahedral while Al_4C^- is planar, so the adiabatic transition requires a large geometry deformation. Indeed, according to our calculations, the adiabatic detachment energy (ADE) is 1.93 eV [CCSD(T)/6-311+G(2df)], which is substantially smaller than the 2.71 eV VDE. Feature X was observed as a structureless band in the PES spectra (Figure 1) because the experimental resolution was not sufficient to resolve the low-frequency vibrations in this band. Thus, the ADE could not be reliably obtained experimentally, as is clear from the long tail of the PES spectra at the low binding energy side (Figure 1). The calculated ADE of 1.93 eV is consistent with the onset of the PES signal around 2 eV, as seen from Figure 1.

Features A, B, and C. Removal of an electron from the $2e_u$ MO (HOMO-1) of Al_4C^- leads to a ($1a_{1g}^2 1e_u^4 2a_{1g}^2 1a_{2u}^2 1b_{1g}^2 2e_u^3 1b_{2g}^1 1e_g^0$) electronic configuration for the Al_4C neutral, which can result in both a triplet and a singlet state. The theoretical methods employed in this work do not allow us to rigorously calculate the singlet state (because of the muticonfigurational character of the reference wave function), but the triplet state can be treated with more reasonable accuracy. According to our CCSD(T)/6-311+G(2df) calculations, the VDE leading to the triplet state is 2.88 eV, which is in excellent agreement with experimental feature A (Figure 1) at 2.86 eV. We therefore assign this peak to removal of an electron from the $2e_u$ orbital (HOMO-1) to produce triplet Al_4C. This $2e_u$ orbital is a primarily nonbonding MO (Figure 3) and is composed of a 2p AO of carbon and 3s−3p hybridized AOs of the aluminum atoms. The removal of the $2e_u$ electron results in a triplet state, which is Jahn−Teller unstable and splits into two components as the Al_4 square distorts into a diamond shape. We therefore assign feature B at 3.00 eV to be the second component of this Jahn−Teller splitting of the triplet state.

The fourth detachment feature (peak C, Figure 1), observed at 3.3 eV VDE (Table 4), is assigned to the singlet state resulting from removing an electron from the same $2e_u$ MO. This feature and features A and B are all considerably sharper than the ground-state feature X. The relative sharpness of these three detachment channels suggests that the geometry changes are smaller upon removal of a $2e_u$ electron from Al_4C^- and that the corresponding neutral states may possess similar quasiplanar structures as that of the anion. This is understandable because removing an electron from the $2e_u$ orbital only weakly disturbs the quasiplanar geometry, although it may induce some excita-

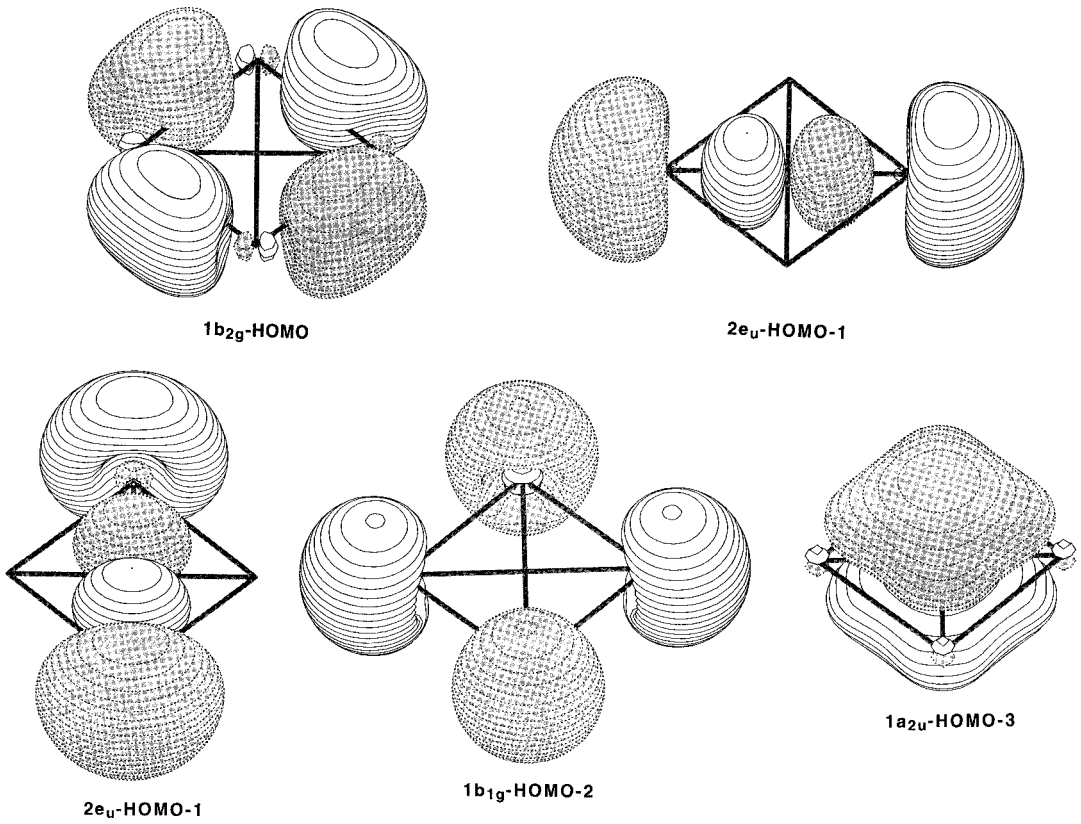

Figure 3. Molecular orbital pictures for D_{4h} Al_4C^-, showing the HOMO ($1b_{2g}$), HOMO-1 ($2e_u$), HOMO-2 ($1b_{2g}$), and HOMO-3 ($1a_{2u}$).

Table 4. Calculated and Experimental Electron Detachment Processes of Al_4C^- (D_{4h}, $^2B_{2g}$, $1a_{1g}^2 1e_u^4 2a_{1g}^2 1a_{2u}^2 1b_{1g}^2 2e_u^4 1b_{2g}^1 1e_g^0$)

state	exptl VDE (eV)	electron detachment from MO	theoretical VDE[a] (eV)	theoretical ADE[a] (eV)
X	2.65(6)	$1b_{2g}$[b]	2.71	1.93
A	2.86(6)	$2e_u$[c]	2.88	
B	3.00(6)	$2e_u$[d]		
C	3.30(6)	$2e_u$[b]		
D	~3.7	$1b_{1g}$[c]	3.77	
E	~4.2	$1a_{2u}$[c]	4.30	

[a] At the CCSD(T)/6-311+G(2df) level of theory with CCSD(T)/6-311+G* geometry. [b] Final singlet state. [c] Final triplet state. [d] Due to Jahn−Teller splitting of the triplet state.

tion of Al−C stretching modes because of its small antibonding nature. More importantly, the $1b_{2g}$ MO, which is important for planarity, is still occupied in all three detachment channels.

Feature D. According to the $1a_{1g}^2 1e_u^4 2a_{1g}^2 1a_{2u}^2 1b_{1g}^2 2e_u^4 1b_{2g}^1 1e_g^0$ ground-state configuration of Al_4C^-, the next detachment channel should involve removal of a $1b_{1g}$ electron, resulting in two states $^3A_{2g}$ and $^1A_{2g}$ ($1a_{1g}^2 1e_u^4 2a_{1g}^2 1a_{2u}^2 1b_{1g}^1 2e_u^4$ $1b_{2g}^1 1e_g^0$). Our CCSD(T)/6-311+G(2df) calculations yielded a VDE for the $^3A_{2g}$ final state of 3.77 eV, which is in excellent agreement with feature D at ~3.7 eV (Figure 1b). The $1b_{1g}$ orbital is a nonbonding MO composed primarily of the 3s AO of aluminum atoms with some hybridization with the 3p AO (Figure 3). For the reason we discussed earlier, we could not calculate the singlet open-shell $^1A_{2g}$ state, which might correspond to the weak feature observed near 3.9 eV.

Feature E. The next detachment channel should be due to the removal of an electron from the $1a_{2u}$ MO, which is weakly C−Al π-bonding and mainly composed of the out-of-plane p_z AO from the central C with some π-bonding from the p_z AOs of the ligands (Figure 3). Again, removing an electron from this MO results in two states, $^3B_{1u}$ and $^1B_{1u}$. According to our CCSD(T)/6-311+G(2df) calculations, the VDE for the $^3B_{1u}$ final state is found to be 4.30 eV, which is in good agreement with the experimental value obtained for feature E (Figure 1). The PES features at higher binding energies were especially complicated and less well resolved. Nevertheless, the qualitative agreement between the calculation and the experiment lends strong support for this assignment for feature E.

Discussion

The overall agreement between the experimental PES spectra and the theoretical calculations is quite satisfying. Despite the apparent complexity of the PES spectra of Al_4C^-, the calculations allowed us to make semiquantitative assignments of all the major spectral features. In particular, the excellent agreement between the calculations and the experiment on the energy and broadness of the transition to the ground state of Al_4C provides strong support for the planar structure of the Al_4C^- anion and the tetrahedral structure for the Al_4C neutral. The quasiplanarity of Al_4C^- indicates that occupation of the ligand−ligand bonding MO, $1b_{2g}$, is critical to achieving planar geometry. As a result, excited states of Al_4C involving occupation of the $1b_{2g}$ MO are also likely to be planar or quasiplanar. The relative sharpness of the photodetachment features corresponding to the A, B, C, and D (Figure 1) features is consistent with this observation and suggests that these neutral states may in fact be planar.

The high vertical and adiabatic electron detachment energies of Al_4C^- (2.65 and 1.93 eV, Table 4) show the strong ligand−ligand bonding in the $1b_{2g}$ HOMO which is composed of electropositive aluminum orbitals (Figure 3). We can estimate the strength of this bonding by comparing the electron affinity

of atomic Al (0.441 ± 0.10 eV[38]) with the 1.93 eV adiabatic EA of Al_4C. The difference between 1.93 and 0.44 eV represents the strong stabilization arising when the aluminum ligand atoms interact to form the $1b_{2g}$ HOMO and then produce the 1-electron, four-center chemical bond.

We calculated the vertical electron attachment energy (VEAE) of an electron into the 1e LUMO at the T_d structure of neutral Al_4C using the OVGF/6-311+G(2df) level of theory. This VEAE (0.93 eV) obtained is much smaller than the 1.93 eV adiabatic electron attachment energy (AEAE), showing the importance of planarization upon formation of Al_4C^- to achieving maximum stabilization in the bonding.

These findings suggest that a wide variety of planar molecules with 17 or 18 valence electrons can be designed. Several such planar molecules have already been predicted theoretically by replacing two of the ligand Al atoms with Si or Ge.[6] The central C can also be replaced to achieve planarity. We noted that Al_4N and Al_4N^-, which have been studied previously, are both planar.[21,22] The latter is particularly interesting because the anion Al_4N^- has 18 valence electrons with a closed shell electron configuration, which should result in simple PES spectra because only doublet final states can be accessed. That was indeed born out in our previous PES study.[22] Planar molecules involving other central atoms, such as Si, P, or Ge, are likely to exist and would be extremely interesting to investigate.

(37) MO pictures were made with MOLDEN3.4 program. G. Schaftenaar, MOLDEN3.4; CAOS/CAMM Center, The Netherlands,1998.

(38) Hotop, H.; Lineberger, W. C. J. *Phys. Chem. Ref. Data* **1985**, *14*, 731.

Conclusions

The pentaatomic Al_4C^- molecule with a tetracoordinated planar carbon (averaged over the zero-point energies) was experimentally observed for the first time. Planarity in Al_4C^- is achieved through ligand−ligand bonding interactions in the HOMO. While the central cavity in the Al_4C^- anion is a bit too small to accommodate the carbon atom at the potential energy surface minimum, vibrational averaging results in an essentially planar structure. To achieve perfect planarity at the potential energy surface minimum, one can use larger ligands such as Ga, Ge, In, or Sn to better accommodate the carbon atom in the center of the cavity. We also expect that neutral pentaatomic molecules, such as CAl_3Si, CAl_2GaSi, $CAlGa_2Si$, CGa_3Si, or CAl_3Ge, should be good candidates for further search for pentaatomic species with planar carbon.

Acknowledgment. The theoretical work done in Utah is supported by the National Science Foundation (CHE-9618904). The authors acknowledge the Center for High Performance Computations at the University of Utah for computer time. The experimental work done in Washington is supported by the National Science Foundation (DMR-9622733). The experiment was performed at the W. R. Wiley Environmental Molecular Sciences Laboratory, a national scientific user facility sponsored by DOE's Office of Biological and Environmental Research and located at Pacific Northwest National Laboratory, which is operated for DOE by Battelle under Contract DE-AC06-76RLO 1830. L.S.W. is an Alfred P. Sloan Foundation Research Fellow.

JA9906204